

Electronic Supplementary Information

for

**Enclosure of a Keggin-type heteropolyoxometalate into a tubular  $\pi$ -space *via* hydrogen bonds with a nonplanar Mo(V)-porphyrin complex forming a supramolecular assembly**

Atsutoshi Yokoyama, Takahiko Kojima\* and Shunichi Fukuzumi\*

*Department of Material and Life Science, Division of Advanced Science and Biotechnology, Graduate School of Engineering, Osaka University, ALCA, Japan  
Science and Technology Agency (JST), Suita, Osaka 565-0871, Department of Chemistry, Graduate School of Pure and Applied Sciences, University of Tsukuba, Tsukuba, Ibaraki 305-8571 and Department of Bioinspired Science, Ewha Womans University, Seoul 120-750, Korea*

\* To whom correspondence should be addressed.

E-mail: [kojima@chem.tsukuba.ac.jp](mailto:kojima@chem.tsukuba.ac.jp), [fukuzumi@chem.eng.osaka-u.ac.jp](mailto:fukuzumi@chem.eng.osaka-u.ac.jp)

**X-ray Crystallography. X-ray crystallography on 1.** A single crystal of **1** was coated in liquid paraffin and mounted on a glass fiber with silicon grease. X-ray diffraction data were collected on a Rigaku Mercury CCD at  $170 \pm 2$  K. All calculations for structure refinements were carried out on a personal computer using *CrystalStructure* (Rigaku Corp., Japan)<sup>1</sup> and SHELXL programs.<sup>2</sup>

**Structure Refinements for 1 and 3.** Refinements on  $F^2$  were performed for all reflections. The weighted  $R$  factor ( $R_w$ ) and goodness of fit ( $S$ ) are based on  $F^2$ , and the conventional  $R$  factor ( $R$ ) on  $F$ , with  $F$  set to zero for negative  $F^2$ . The threshold expression of  $F^2 > 2\sigma(F^2)$  was used only for calculating  $R$  factors (gt) etc. and was not relevant to the choice of reflections for refinement.  $R$  factors based on  $F^2$  are statistically about twice as large as those based on  $F$ , and  $R$  factors based on all data are even larger. As for **3**, the restraint program “ISOR S1” was used for the refinement.

- (1) *CrystalStructure 3.7.0*: Crystal Structure Analysis Package, Rigaku and Rigaku/MSK (2000-2005), The Woodlands, TX 77381, USA.
- (2) *SIR 97* and *SHELX 97*: G. M. Sheldrick, *Program for Crystal Structures Refinement*, University of Göttingen, Germany, 1997.

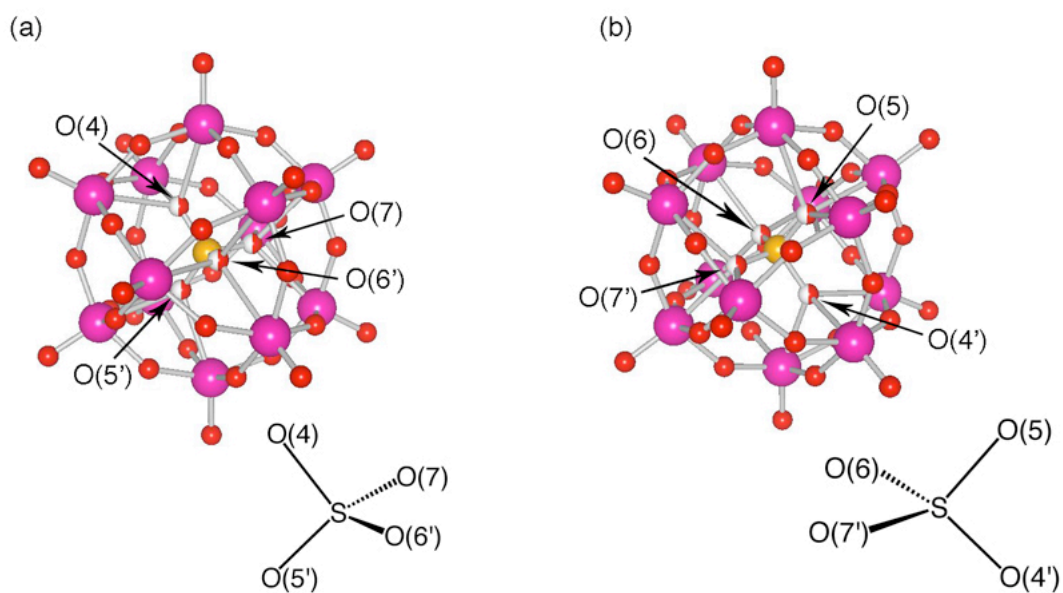


**Fig. S1** Disordered two tetrahedrons around the sulfur atom in the Keggin structure.  
Red, oxygen; red and white, disordered oxygen; pink, tungsten; orange, sulfur.

**Table S1.** Selected bond distances (Å), interatomic distances (Å) and bond angles (deg) for **3**.

assignment	<b>3</b>	
	distance (Å)	angle (deg)
Mo(1)-O(1)	1.671(6)	—
Mo(1)-O(2)	2.371(6)	—
O(2)-O(3)	2.87(1)	—
O(2)-O(25A)	3.01(3)	—
O(25A)-O(25A')	3.22(2)	—
W(1)-O(3)	1.679(6)	—
S(1)-O(4)	1.52(1)	—
S(1)-O(5)	1.48(1)	—
S(1)-O(6)	1.46(1)	—
S(1)-O(7)	1.40(1)	—
Mo(1)-O(2)-O(3)	—	112.9(2)
O(2)-O(3)-W(1)	—	152.5(4)
O(3)-O(2)-O(25A)	—	116.2(2)
O(2)-O(25A)-O(25A')	—	105.9(7)

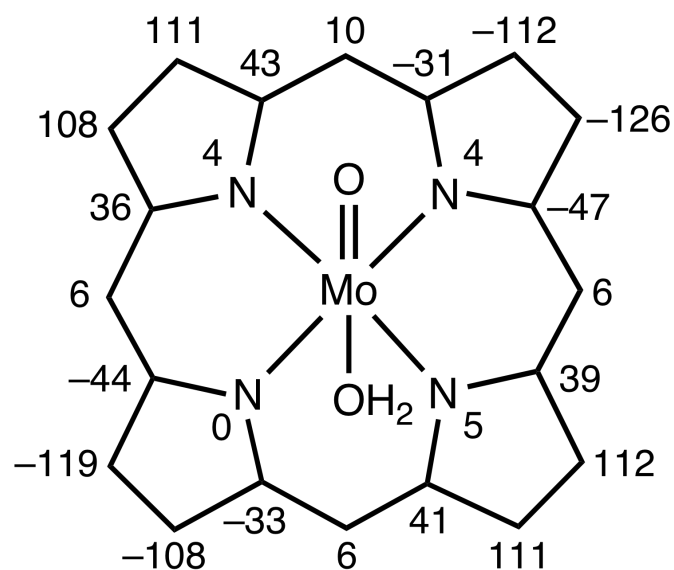


**Fig. S2** The displacement of each atom from the least-squares mean plane of 24 atoms of the DPP<sup>2-</sup> moiety in **3** (in unit of 0.01 Å).

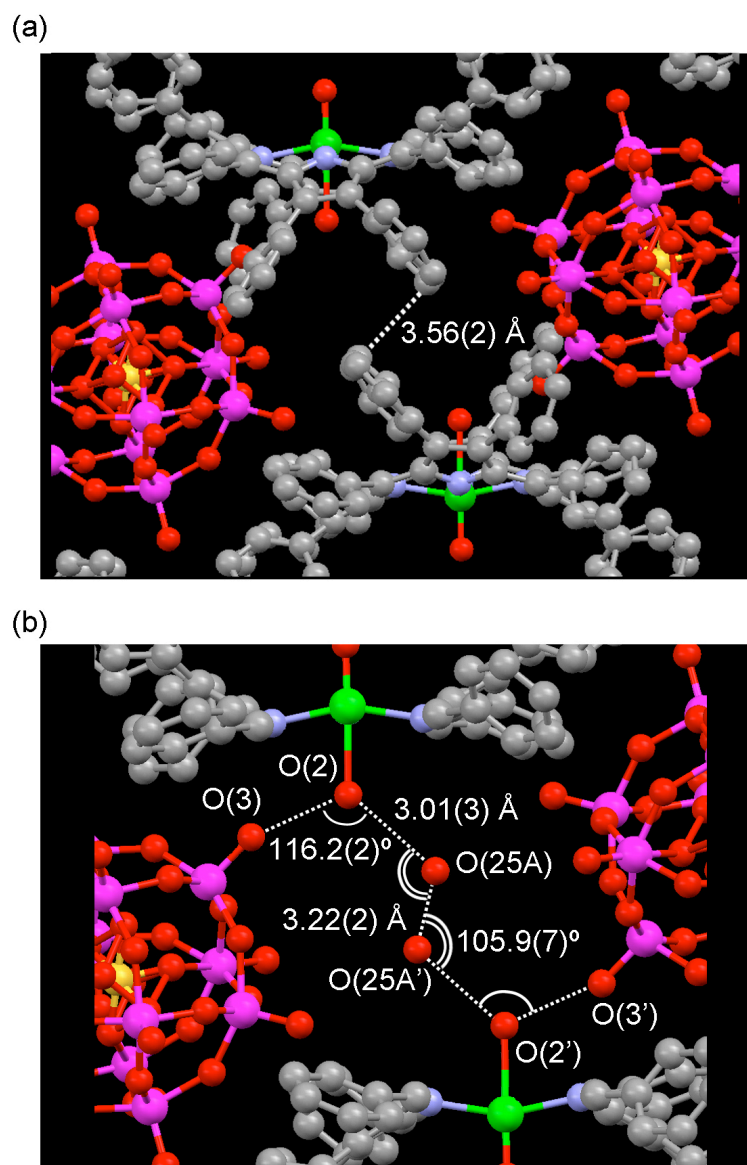


**Fig. S3** (a) Intermolecular  $\pi$ - $\pi$  interaction between peripheral phenyl groups of two Mo(V)-porphyrin units. (b) A hydrogen bonding network involving water molecules of crystallization (O(25)). Gray, carbon; blue, nitrogen; red, oxygen; green, molybdenum; pink, tungsten; orange, sulfur.

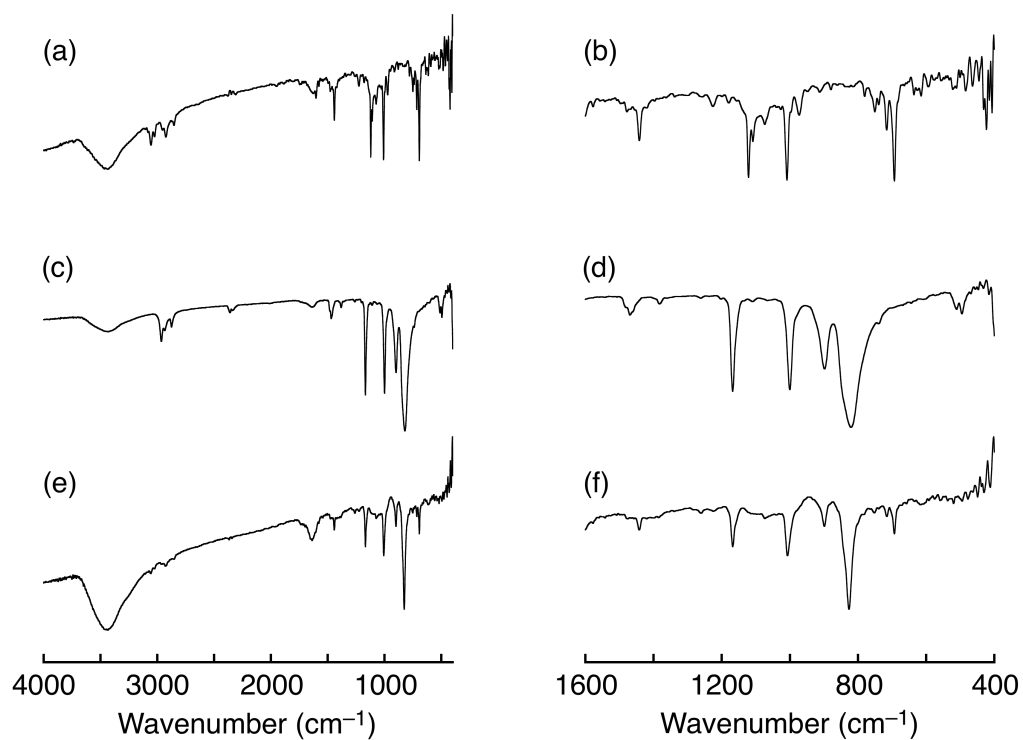


**Fig. S4** IR spectra (KBr) of **1** ((a), (b)), **2** ((c), (d)) and **3** ((e), (f)).

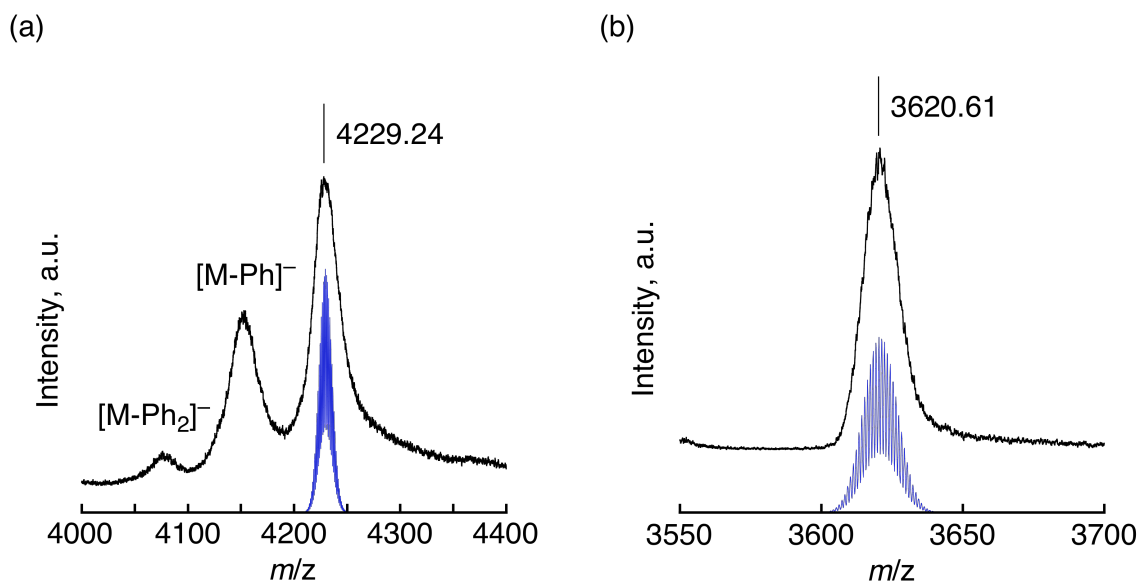


**Fig. S5** (a) MALDI-TOF-MS spectrum of **4** ( $m/z = 4229.24$ ) and computer simulation ( $[\{\text{Mo}(\text{DPP})(\text{O})(\text{H}_2\text{O})(\text{SW}_{12}\text{O}_{40})\}]^-$ , 4229.59  $m/z$ ] in  $\text{CH}_2\text{Cl}_2$ . (b) MALDI-TOF-MS spectrum of **6** ( $m/z = 3620.61$ ) and computer simulation ( $[\{\text{Mo}(\text{TPP})(\text{O})(\text{H}_2\text{O})(\text{SW}_{12}\text{O}_{40})\}]^-$ , 3620.81  $m/z$ ] in  $\text{CH}_2\text{Cl}_2$ . (linear negative mode, matrix;  $\alpha$ -cyano-4-hydroxycinnamic acid (CHCA)).



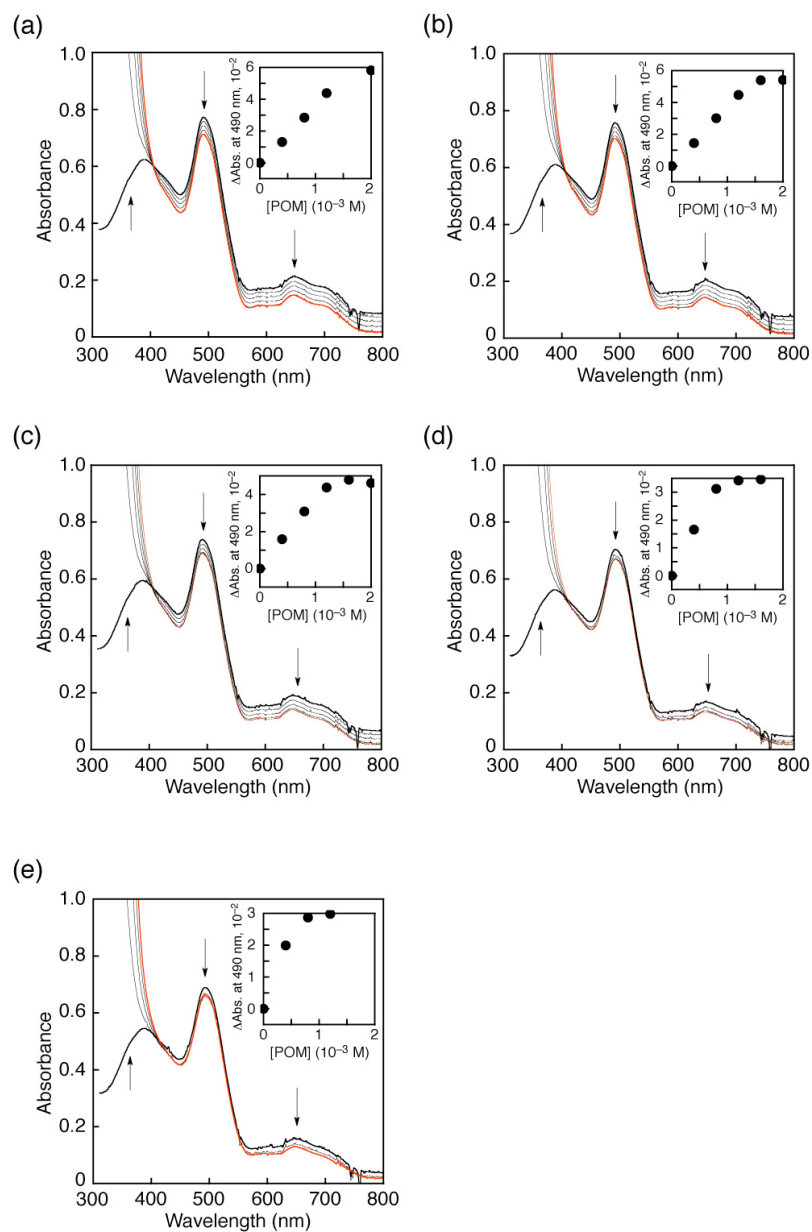


**Fig. S6** UV-vis spectral titration of **1** ( $1.0 \times 10^{-5}$  M) upon addition of **2** in PhCN at 265 K (a), 273 K (b), 283 K (c), 303 K (d) and 313 K (e). Each  $\Delta\text{Abs}$  ( $A - A_0$ ) at 490 nm was plotted as insets.

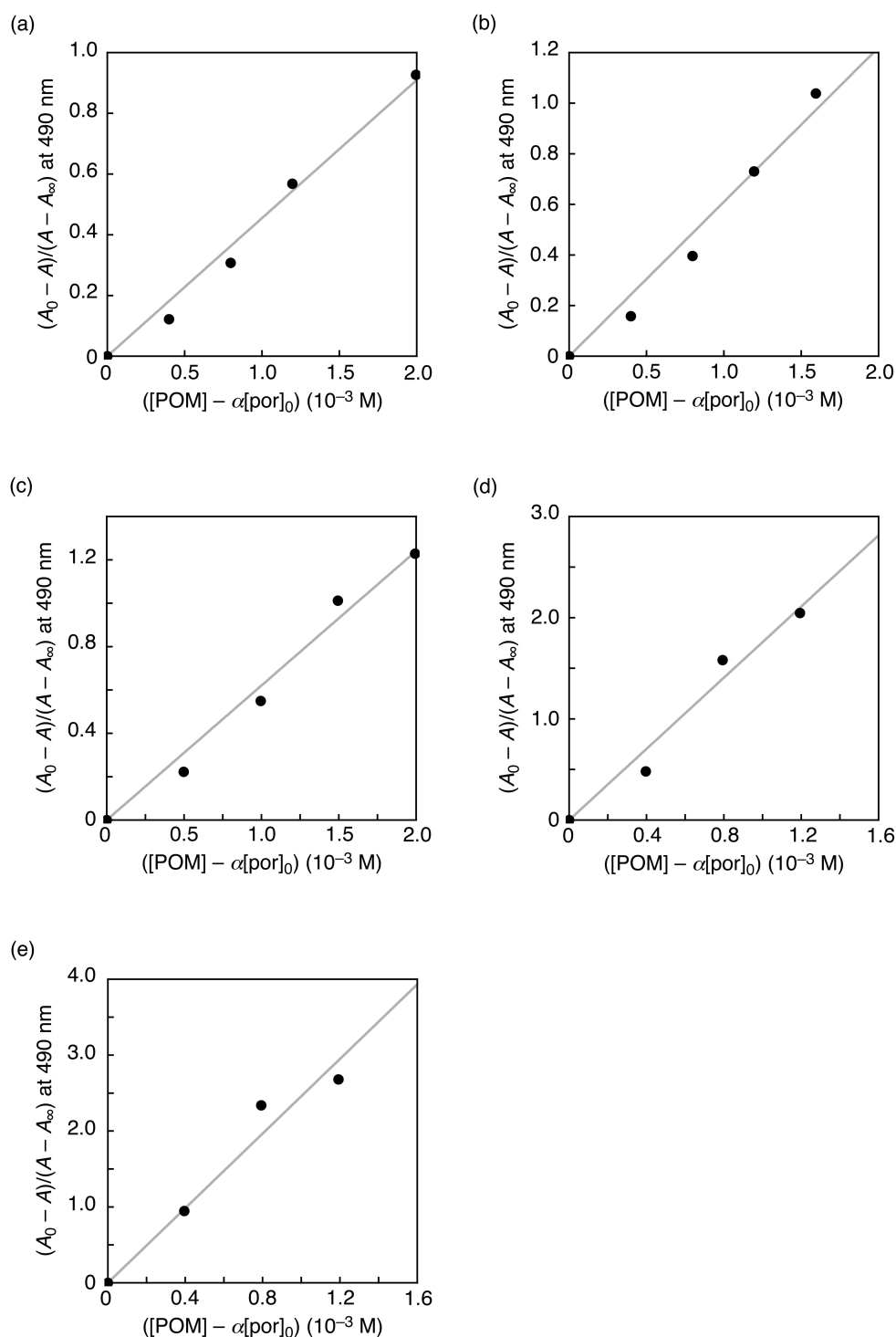


**Fig. S7** Plots of  $(A - A_0)/(A_\infty - A)$  versus  $([POM] - \alpha[por]_0)$  for the spectroscopic titration of **1** upon addition of **2** in PhCN using absorbance at 490 nm; (a) 265 K, (b) 273 K, (c) 283 K, (d) 303 K and (e) 313 K.

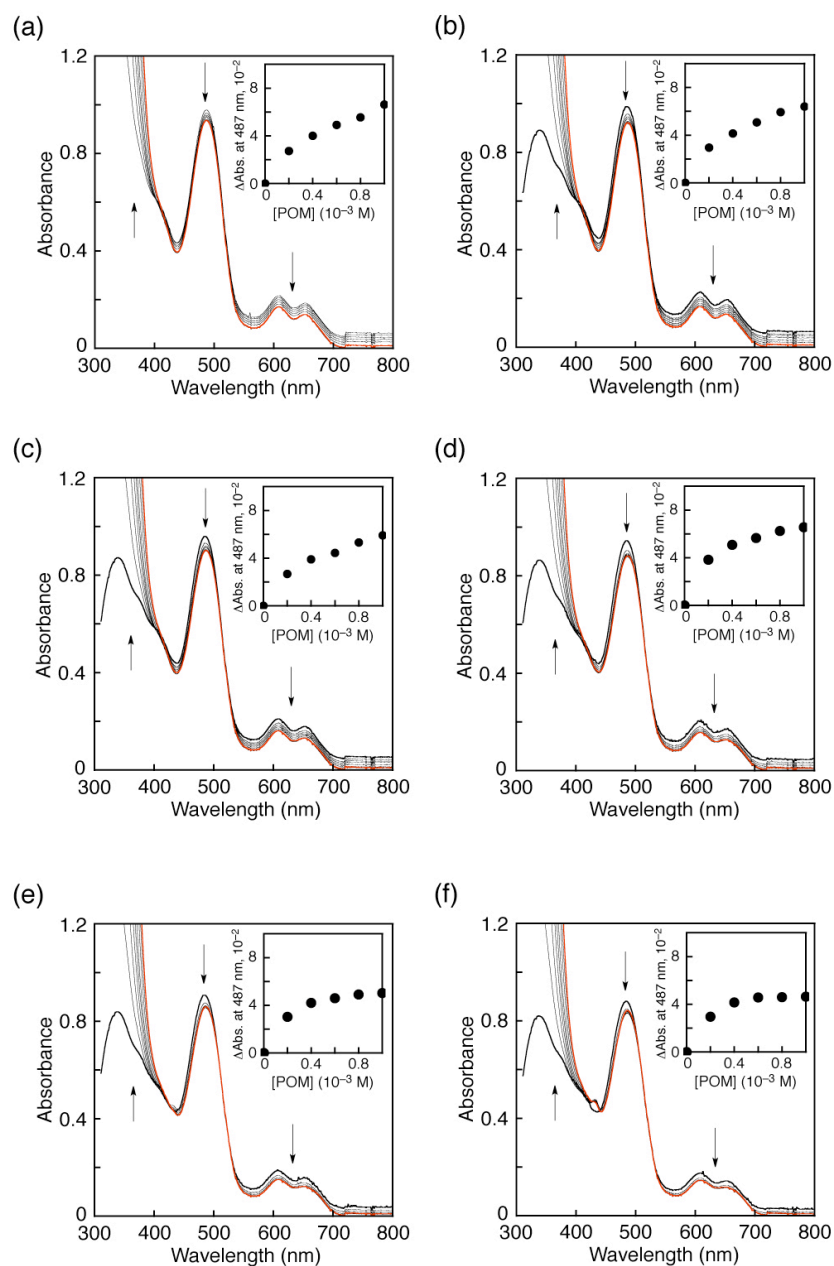


**Fig. S8** UV-vis spectral titration of **4** ( $2.0 \times 10^{-5}$  M) upon addition of **2** in PhCN at 265 K (a), 273 K (b), 283 K (c), 293 K (d), 303 K (e) and 313 K (f). Each  $\Delta\text{Abs}$  ( $A - A_0$ ) at 487 nm was plotted as insets.

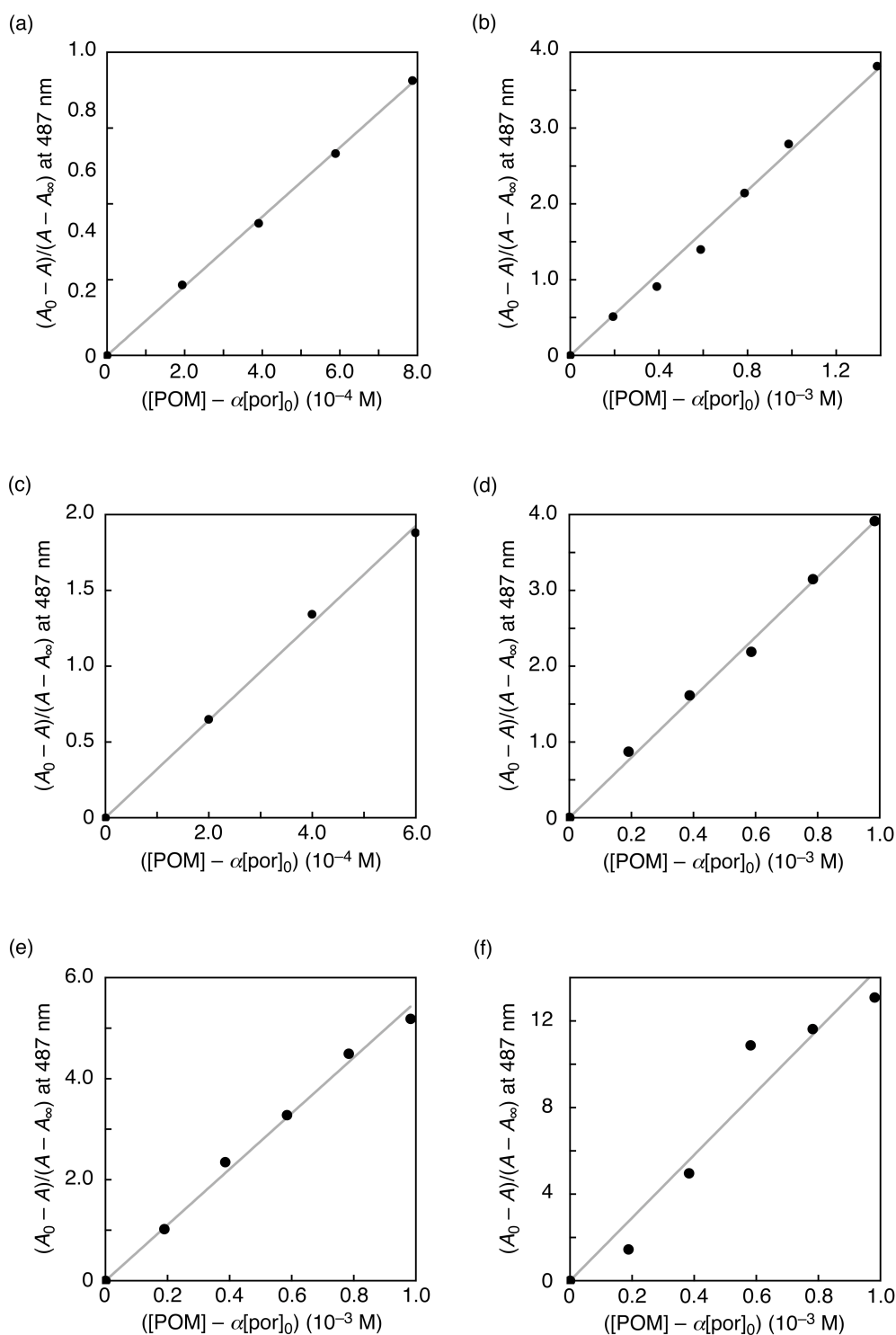


**Fig. S9** Plots of  $(A - A_0)/(A_\infty - A)$  versus  $([POM] - \alpha[por]_0)$  for the spectroscopic titration of **4** upon addition of **2** in PhCN using absorbance at 487 nm; (a) 265 K, (b) 273 K, (c) 283 K, (d) 298 K, (e) 303 K and (f) 313 K.

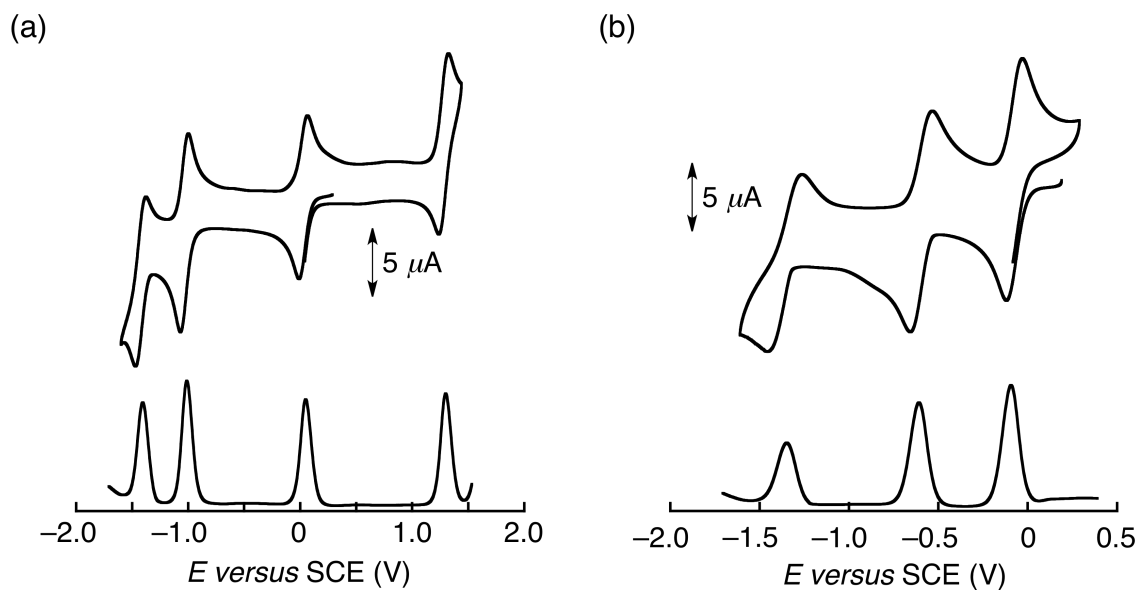


**Fig. S10** Cyclic voltammograms (upper) and differential pulse voltammograms (bottom) for (a) **1** (1.0 mM) and (b) **2** (1.0 mM) under Ar in the presence of 0.1 M TBAPF<sub>6</sub> in PhCN at room temperature.